Supplementary Information

An Organometallic Building Block Approach to Produce a Multidecker 4*f* Single-Molecule Magnet.

Jennifer J. Le Roy,[†] Matthew Jeletic,[†] Serge I. Gorelsky,[†] Ilia Korobkov,[†] Liviu Ungur,[‡] Liviu F. Chibotaru,[‡] Muralee Murugesu*[,†]

[†]Chemistry Department and the Centre for Catalysis Research and Innovation, University of Ottawa, 10 Marie Curie, Ottawa, ON, K1N 6N5, Canada.
[§]Division of Quantum and Physical Chemistry and INPAC Institute for Nanoscale Physics and Chemistry, Katholieke Universiteit Leuven, Celestijnenlaan, 200F, 3001, Belgium.

Table S1. Contractions of the employed basis sets.

Basis 1	Basis 2
Dy.ANO-RCC...7s6p4d3f1g.	Dy.ANO-RCC...8s7p5d4f2g1h.
Lu.ANO-RCC...7s6p4d3f1g.	Lu.ANO-RCC...7s6p4d3f1g.
Si.ANO-RCC...4s3p.	Si.ANO-RCC...5s4p2d.
C.ANO-RCC...3s2p.	C.ANO-RCC...4s3p2d. (close)
H.ANO-RCC...2s.	C.ANO-RCC…3s2p. (distant)
	H.ANO-RCC...3s2p. (close)
	H.ANO-RCC…2s. (distant)

Table S2. The energies of the eight Kramers doublets arising from the *J*=15/2 atomic ground multiplet of individual Dy(III) ions in Dy_2COT_3.

KD		A1		A2		B1		B2		C1		C2	
		E (cm-1)	g	E (cm-1)	g	E (cm-1)	g	E (cm-1)	g	E (cm-1)	g	E (cm-1)	g
1	g_X	0.000	0.0304	0.000	0.3673	0.000	0.0197	0.000	0.2164	0.000	0.0461	0.000	0.1639
	g_Y		0.0577		0.4445		0.0574		0.2707		0.0798		0.1921
	g_Z		19.7444		19.0077		19.7023		18.6060		19.6401		18.7482
2	g_X	41.145	0.1507	25.317	1.8903	31.719	0.3853	30.398	2.0085	30.917	0.6090	34.074	2.1716
	g_Y		0.2196		2.7510		0.5762		2.6777		0.8834		2.8881
	g_Z		16.9312		16.5790		16.8305		16.3829		16.8363		16.2213
3	g_X	82.285	1.0141	52.958	10.7448	71.355	1.7274	55.763	0.3735	69.398	1.9706	58.267	0.7214
	g_Y		1.8598		6.2891		3.6848		4.6246		4.4567		4.6354
	g_Z		13.7653		0.8604		13.2778		10.7054		12.9603		10.4617
4	g_X	109.102	3.0550	87.830	6.9600	101.751	2.6109	85.724	4.3448	102.093	2.2252	89.678	4.4958
	g_Y		6.8872		5.8906		6.7198		6.0815		6.4997		6.2460
	g_Z		11.2336		0.0805		11.8583		8.8722		11.7475		8.4927
5	g_X	125.401	0.8672	102.433	2.2865	121.310	0.7334	105.426	0.9093	124.709	0.7943	110.116	0.9040
	g_Y		1.2320		5.1226		1.0084		1.7470		0.9363		1.7659
	g_Z		15.5723		11.8265		17.3812		15.4588		16.9155		15.4027
6	g_X	180.193	0.1827	126.058	0.1809	155.940	0.3248	134.362	0.0981	147.778	0.4621	138.828	0.1141
	g_Y		0.2560		0.3600		0.4928		0.2668		0.8713		0.2842
	g_Z		14.3282		19.2895		14.1476		19.1948		13.9718		19.2445
7	g_X	423.644	0.0012	301.999	0.0036	385.800	0.0020	282.528	0.0075	370.091	0.0020	286.503	0.0065
	g_Y		0.0014		0.0045		0.0025		0.0093		0.0025		0.0083
	g_Z		17.4272		17.4079		17.4166		17.3921		17.4128		17.3929
8	g_X	1126.4	0.0000	951.076	0.0000	1059.593	0.0000	903.145	0.0000	1036.477	0.0000	909.208	0.0000
	g_Y		0.0000		0.0000		0.0000		0.0000		0.0000		0.0000
	g_Z		19.8867		19.8890		19.8867		19.8889		19.8868		19.8889

Table S3. The energies of the eight Kramers doublets arising from the J=15/2 atomic ground multiplet of individual Dy(III) ions in symmetrized Dy_2COT_3 and the symmetrized $DyCOT_2$.

KD		Symmetrized Dy_2COT_3		Symmetrized $DyCOT_2$	
		E (cm^{-1})	*g*	*E* (cm^{-1})	*g*
1	g_X	0.000	**0.1192**	0.000	**10.6675**
	g_Y		**0.1197**		**10.6288**
	g_Z		**11.9622**		**1.3536**
2	g_X	5.915	**10.6073**	15.581	**0.0135**
	g_Y		**10.5710**		**0.0252**
	g_Z		**1.3374**		**4.0364**
3	g_X	7.418	**0.1113**	22.681	**0.0963**
	g_Y		**0.1274**		**0.0966**
	g_Z		**9.2627**		**12.0203**
4	g_X	13.422	**0.0044**	30.542	**0.0392**
	g_Y		**0.0317**		**0.2308**
	g_Z		**3.9971**		**9.3216**
5	g_X	16.935	**0.0053**	31.213	**0.1285**
	g_Y		**0.0223**		**0.1412**
	g_Z		**6.6287**		**6.7009**
6	g_X	50.814	**0.0000**	61.372	**0.0000**
	g_Y		**0.0000**		**0.0000**
	g_Z		**14.7270**		**14.8143**
7	g_X	281.896	**0.0000**	267.320	**0.0000**
	g_Y		**0.0000**		**0.0000**
	g_Z		**17.4749**		**17.5999**
8	g_X	1078.093	**0.0000**	1074.171	**0.0000**
	g_Y		**0.0000**		**0.0000**
	g_Z		**19.8873**		**19.9927**

Table S4. Parameters of the crystal field for the ground multiplet of Dy^{III} ions in Dy_2COT_3.

k	q	Parameter B(k,q)
2	-2	-0.95471346837807E+00
	-1	-0.61290163034954E+00
	0	**0.38452191879230E+01**
	1	-0.43775428702597E+00
	2	-0.28846243887633E+00
4	-4	-0.16911975304825E-02
	-3	0.61509350372093E-03
	-2	-0.15292981075142E-02
	-1	0.34564895212804E-02
	0	**0.16056739351699E-01**
	1	0.24710678545234E-02
	2	0.74363185246023E-04
	3	-0.37017973909043E-02
	4	0.13884232151991E-02
6	-6	-0.76394353456162E-05
	-5	-0.62065816310276E-04
	-4	0.14683989089670E-04
	-3	0.31088685121144E-05
	-2	-0.12772584137055E-04
	-1	0.34389065190826E-05
	0	**0.41255572766156E-04**
	1	0.38204732345991E-05
	2	0.66200061570876E-05
	3	0.58573004580692E-04
	4	-0.12429710317764E-04
	5	-0.20476952360510E-03
	6	-0.28336749023853E-04

Crystal_Field parameters of the ground atomic multiplet computed with SINGLE_ANISO program, using the ab initio results of the computational model C2:
The Crystal-Field Hamiltonian:

$$\mathrm{H}_{CF} = \sum_{k=2,4,6} \sum_{q=-k,k} \left[B_k^q O_k^q \right]$$

where:

O_k^q = Extended Stevens Operators (ESO) as defined in:

1. Rudowicz, C.; J. Phys. C: Solid State Phys.,18(1985) 1415-1430.
2. Implemented in the "EasySpin" function in MATLAB, www.easyspin.org.

k - the rank of the ITO, = 2, 4, 6, 8, 10, 12.
q - the component of the ITO, = -k, -k+1, ... 0, 1, ... k.

Table S5. Selected crystallographic data for **1-3**.

	1	2	3
Torsion angle Si1-COT''$_{centroid1}$-COT''$_{centroid2}$-Si2 (°)	54.98	—	—
Nearest Ln^{III} intermolecular distance (Å)	10.51	9.2	9.03
Ln^{III}- Ln^{III} intramolecular distance (Å)	—	4.14	4.21
Aveerage M-COT''$_{centroid}$ (Å)	1.91	1.79	1.81
Nearest Li-$C_{COT''}$ (Å)	5.62	—	—
Average $C_{COT''}$-Ln^{III} distance (Å)	2.66	2.62	2.65
Si-C (Å)	1.87	1.87	1.87
M_r (g/mol)	936.82	1070.54	1060.04
Formula	$DyC_{40}H_{78}Si_4LiO_6$	$Dy_2C_{42}H_{72}Si_6$	$Gd_2C_{42}H_{72}Si_6$
T(K)	200	200	200
γ (Å)	0.71073	0.71073	0.71073
Crystal system	triclinic	tetragonal	tetragonal
Space group	P-1	I-4	I -4
a (Å)	11.5077(7)	16.8867(5)	16.9774(4)
b (Å)	12.3057(7)	16.8867(5)	16.9774(4)
c (Å)	18.5852(11)	20.1512(6)	20.0097(6)
α (deg)	99.361(3)	90.00	90.00
β (deg)	102.268(3)	90.00	90.00
γ (deg)	99.657(3)	90.00	90.00
V (Å^3)	2481.0(3)	5746.3(3)	5767.44(26)
ρ_{calc} (cm^{-3})	1.254	1.237	1.221
size (mm)	0.19x0.20x0.28	0.11x0.13x0.15 0.14x0.18x0.20	0.16x0.16x0.18
Z	2	4	4
Reflections collected	35322	42231	42421
R(int)	12258, 0.0170	7115, 0.0396	7120,0.0170
R1	0.0177	0.0324	0.0256
wR2	0.0467	0.0827	0.0755
Reflections with $I \geq 2\sigma(I)$	11499	6488	6978

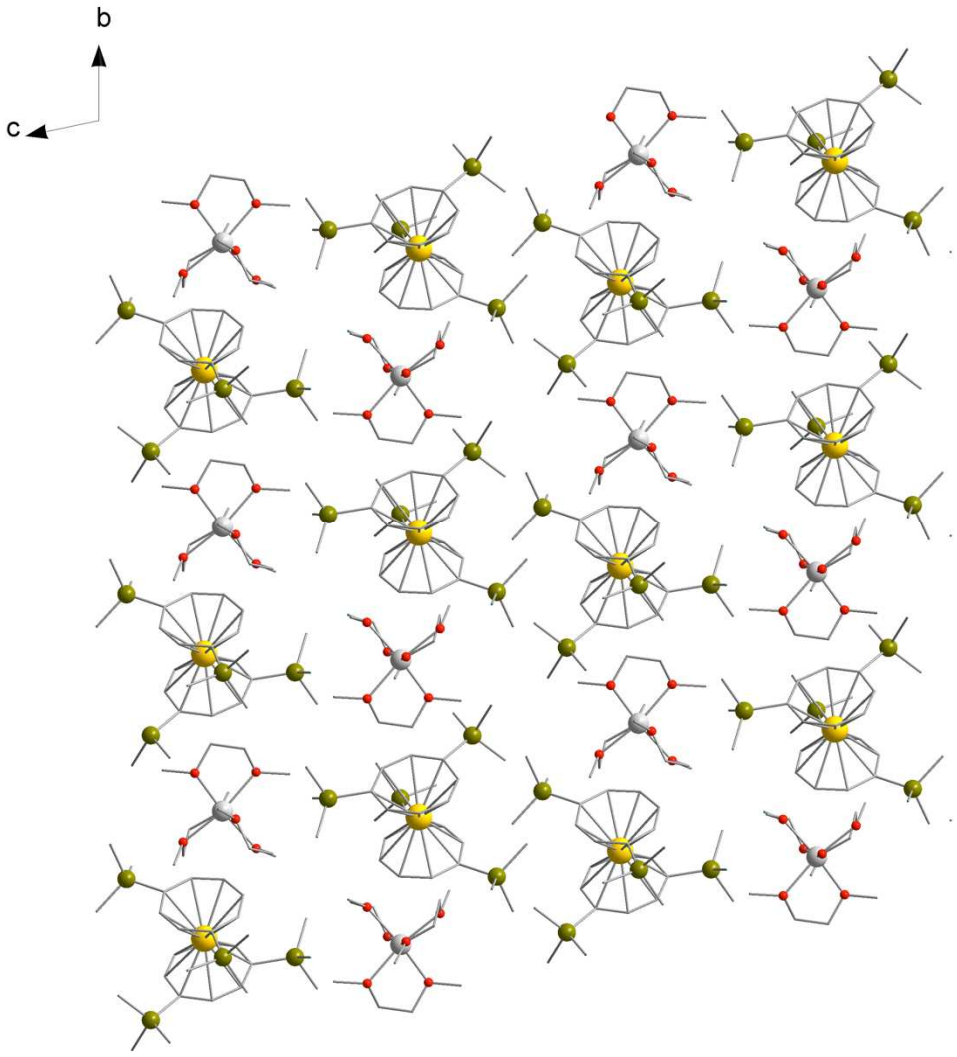

Figure S1: Packing arrangement of **1** looking down the *a* axis. H and C atoms are removed for clarity. Color code: Si = green, Dy = yellow, Li = gray, O = red.

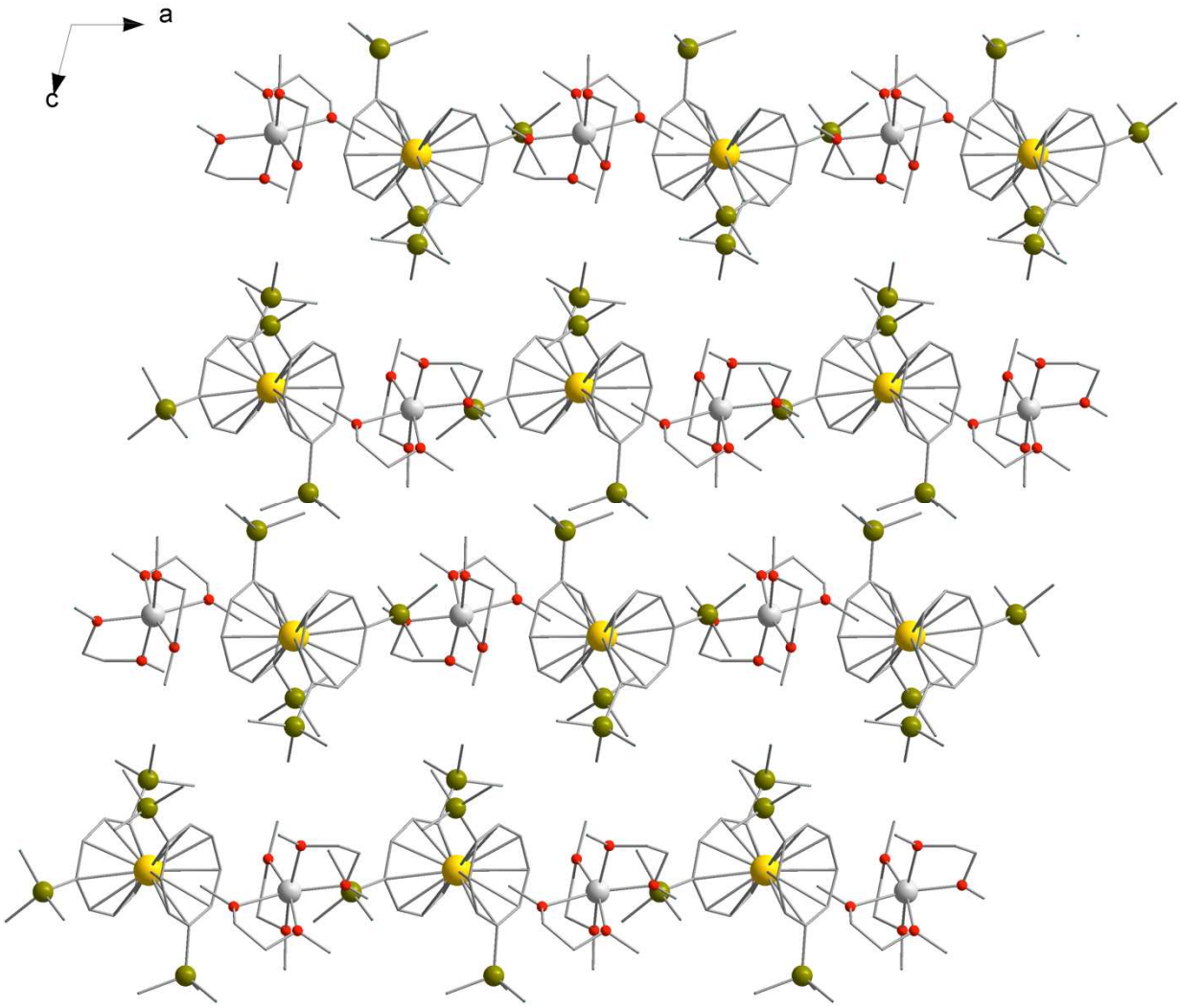

Figure S2: Packing arrangement of **1** looking down the *b* axis. H and C atoms are removed for clarity. Color code: Si = green, Dy = yellow, Li = gray, O = red.

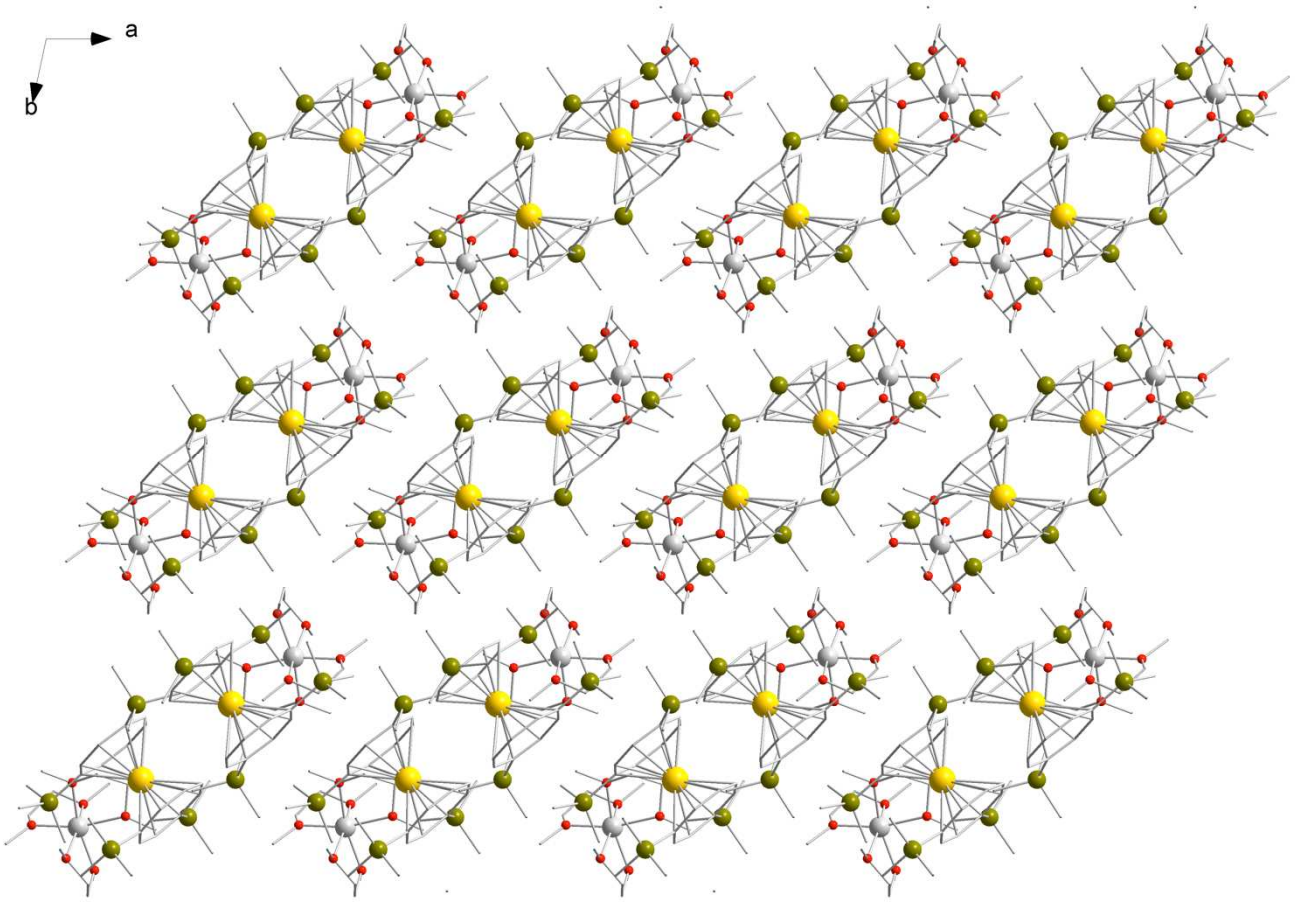

Figure S3: Packing arrangement of **1** looking down the *c* axis. H and C atoms are removed for clarity. Color code: Si = green, Dy = yellow, Li = gray, O = red.

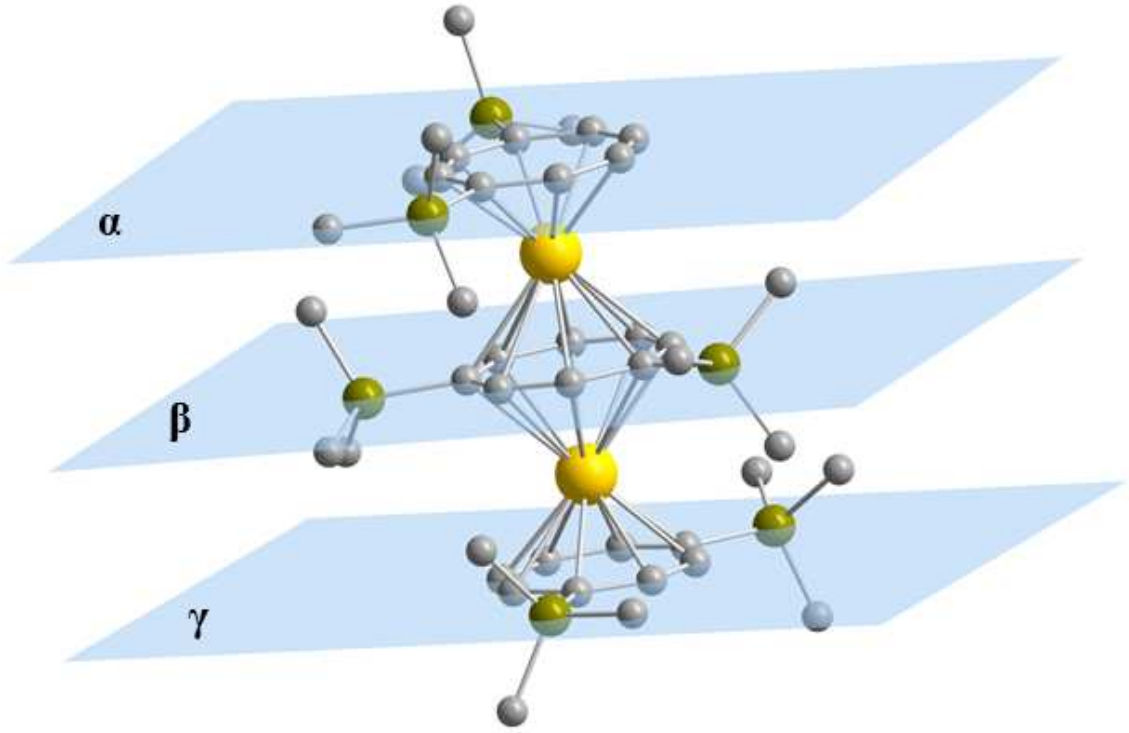

Figure S4: View of **2** with the orientation of the three COT'' planes highlighting the deviation from parallelism. Color code: Si = green, Dy = yellow, C = gray.

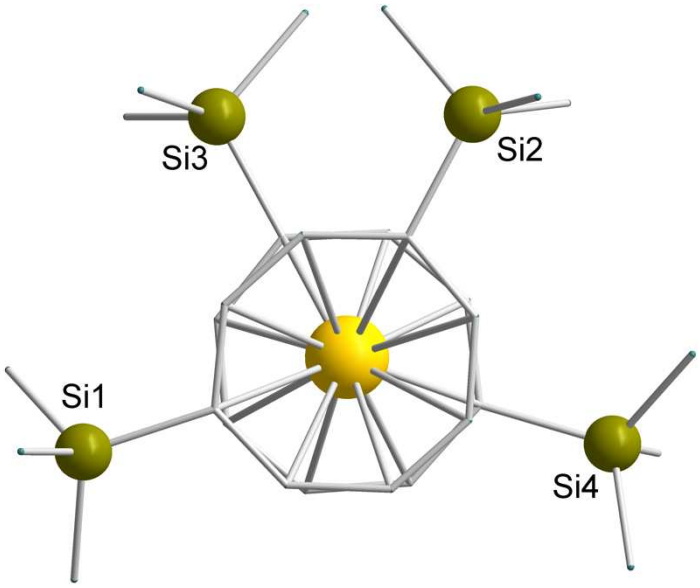

Figure S5: Top-view of **1**. Hydrogen atoms omitted for clarity. Color code: Si = green, Dy = yellow, C = gray.

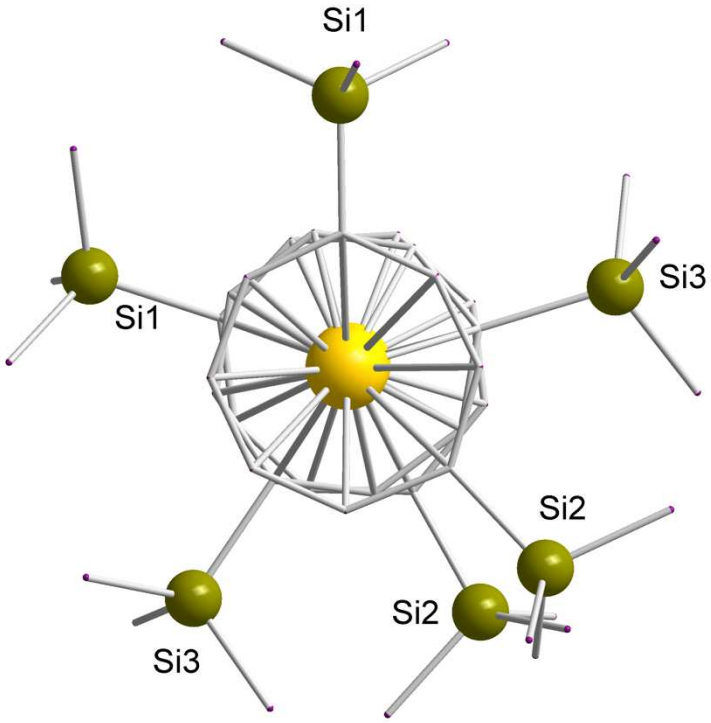

Figure S6: Top-view of **2**. Hydrogen atoms omitted for clarity. Color code: Si = green, Dy = yellow, C = gray.

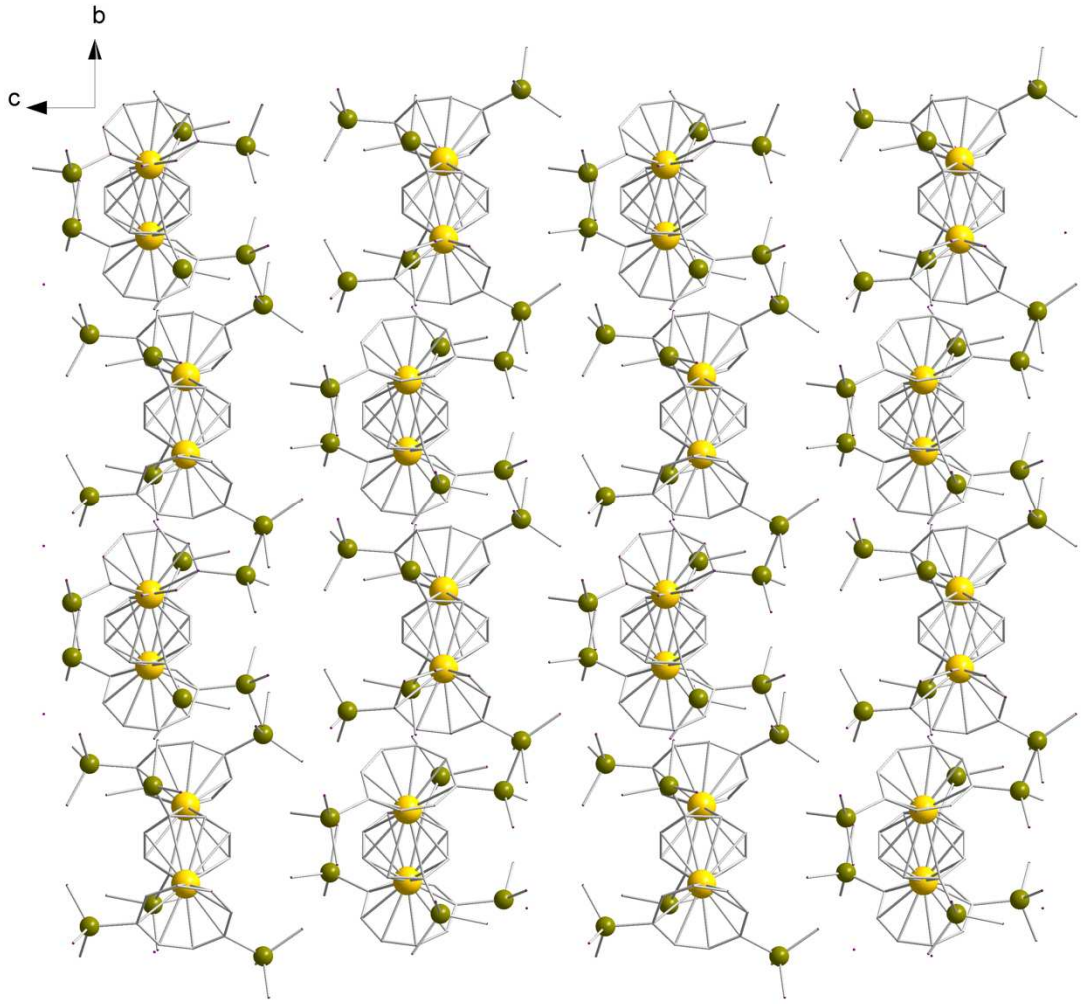

Figure S7: Packing arrangement of **2** looking down the *a* axis. Hydrogen atoms omitted for clarity. Color code: Si = green, Dy = yellow, C = gray.

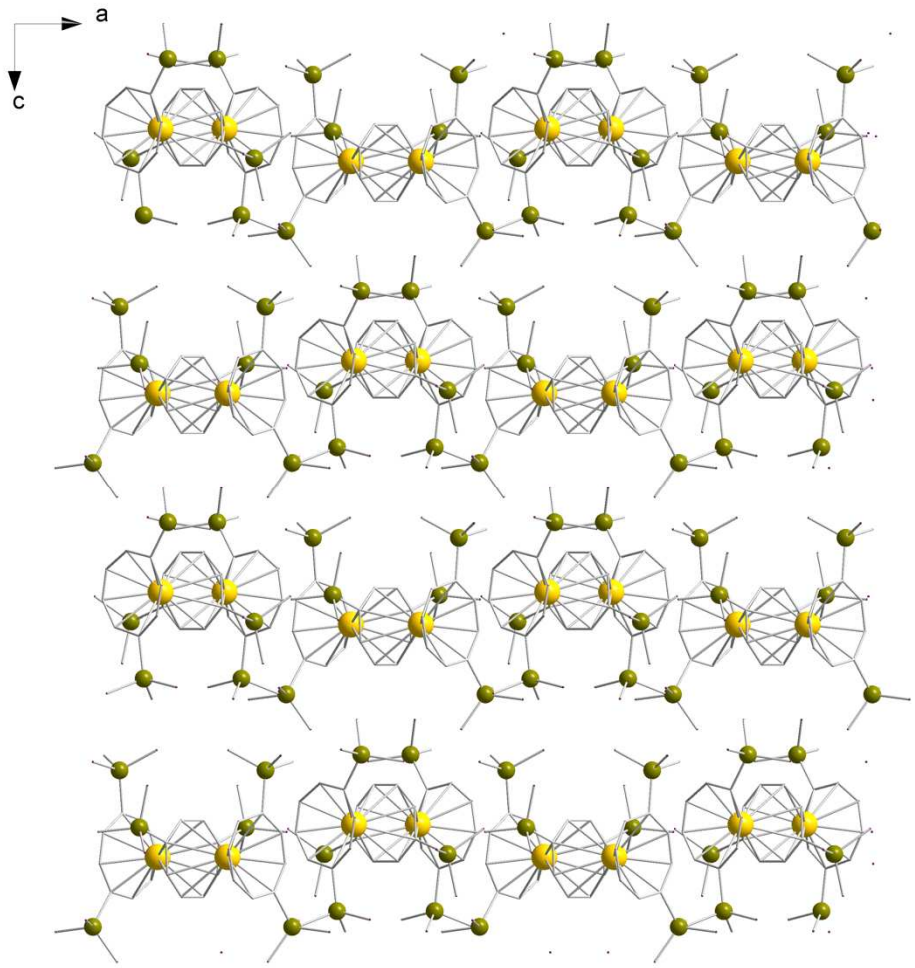

Figure S8: Packing arrangement of **2** looking down the *b* axis. Hydrogen atoms omitted for clarity. Color code: Si = green, Dy = yellow, C = gray.

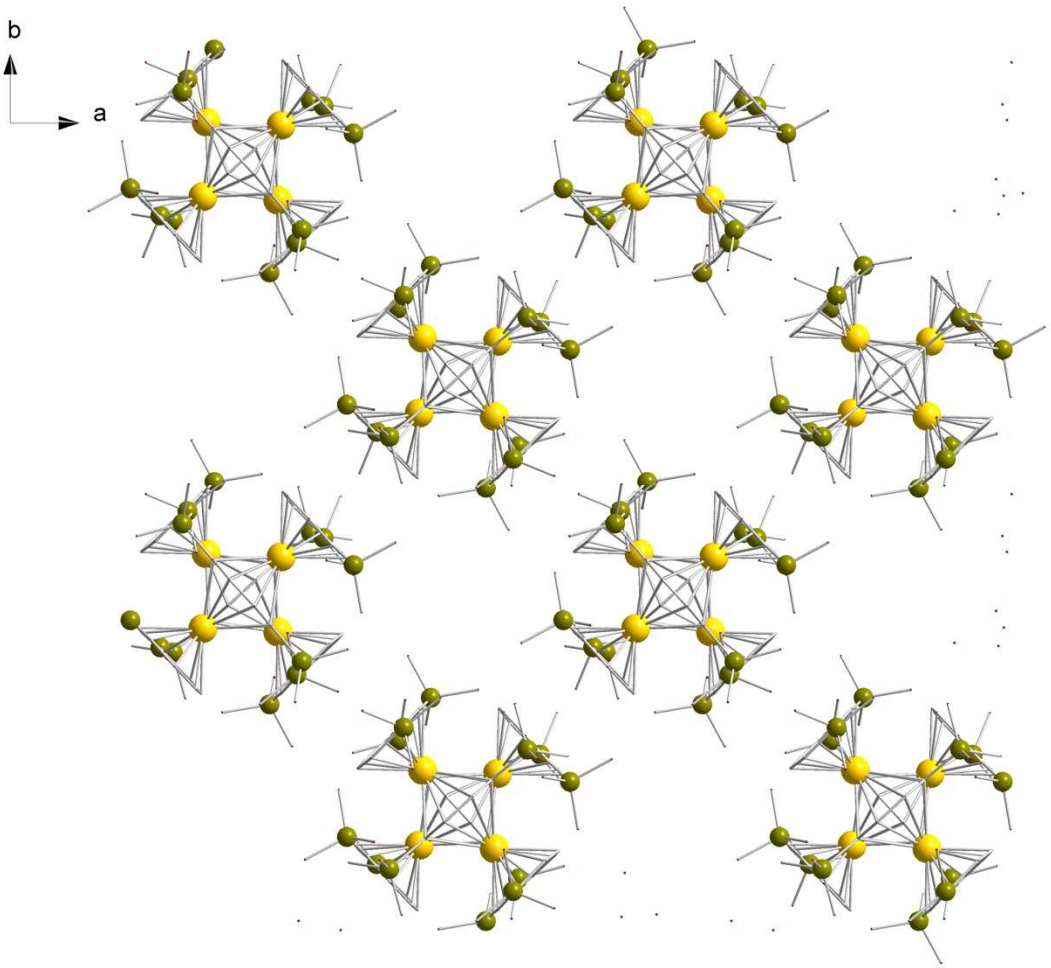

Figure S9: Packing arrangement of **2** looking down the *c* axis. Hydrogen atoms omitted for clarity. Color code: Si = green, Dy = yellow, C = gray.

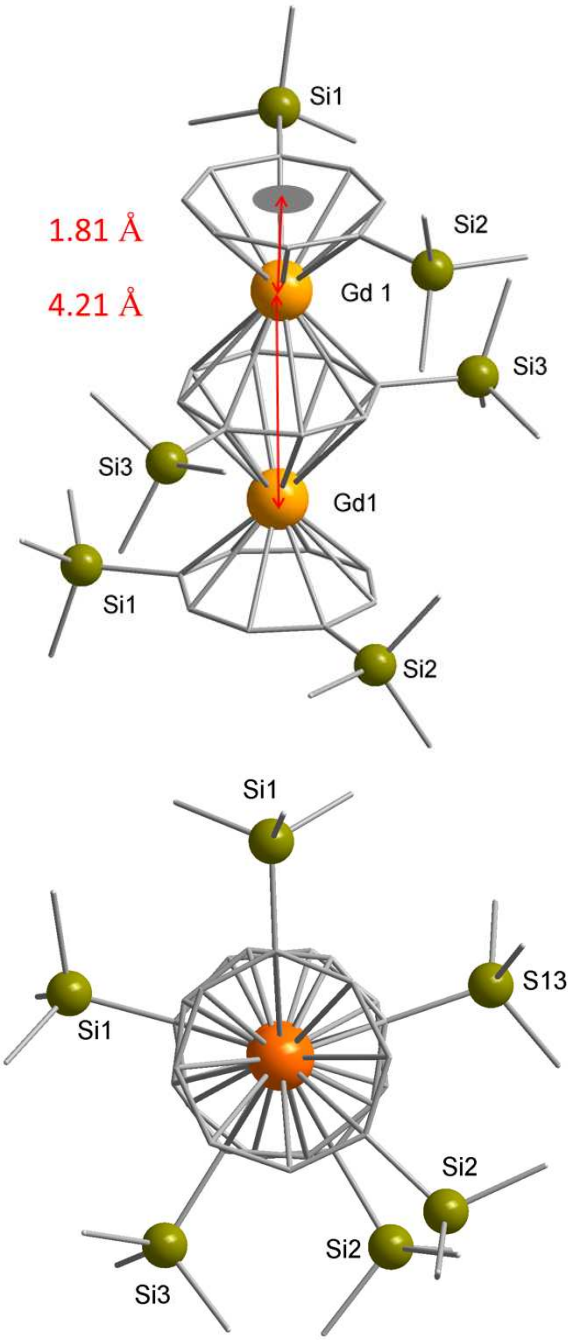

Figure S10: Partially labeled X-ray structures of **3** (top) and top view of **3** (bottom) with H atoms omitted for clarity. Color code: Si = green, Gd = Orange, C = gray.

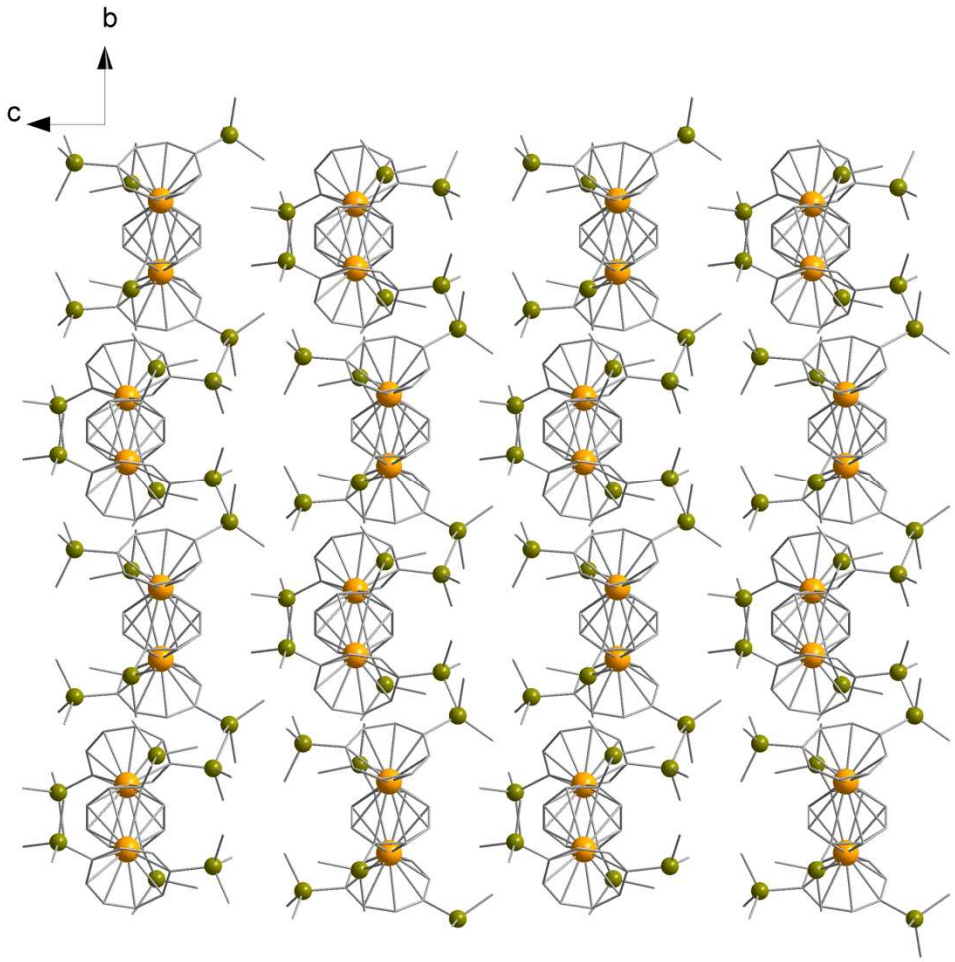

Figure S11: Packing arrangement of **3** looking down the *a* axis. Hydrogen atoms omitted for clarity. Color code: Si = green, Gd = orange, C = gray.

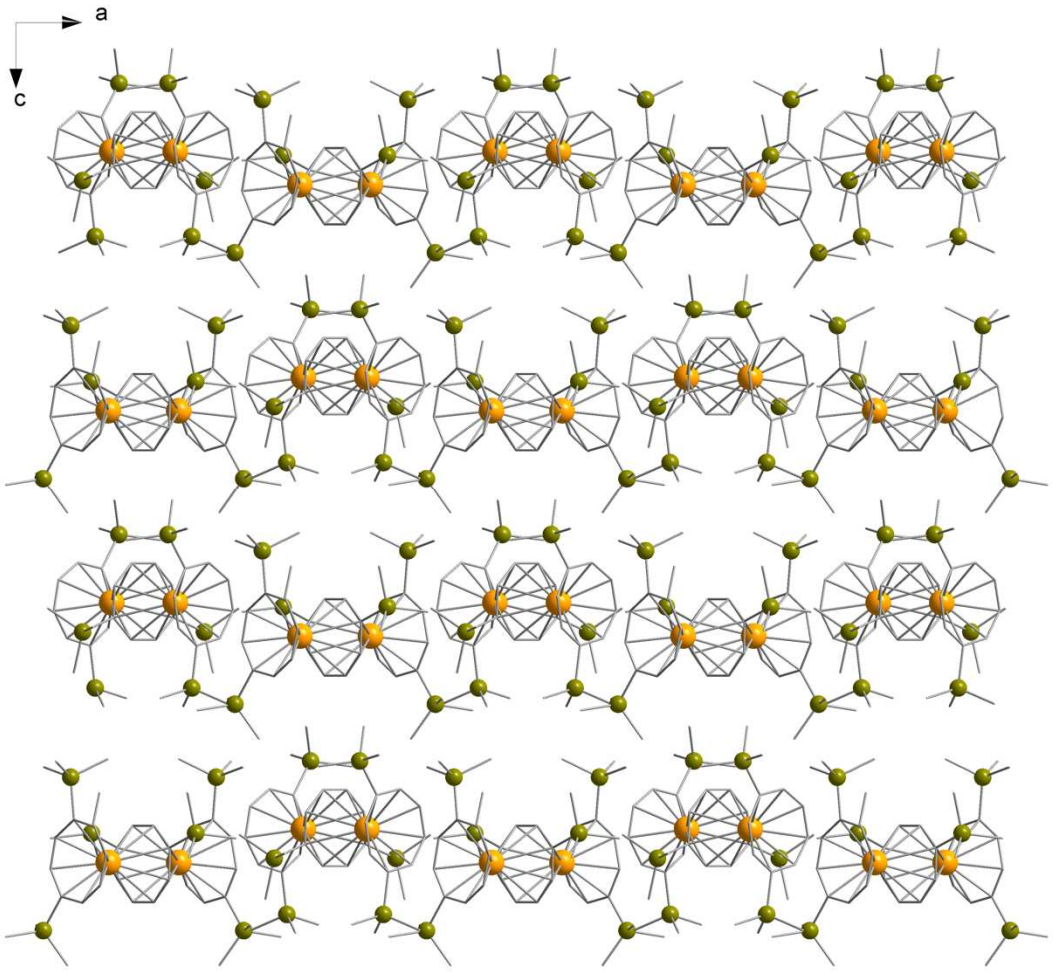

Figure S12: Packing arrangement of **3** looking down the b axis. Hydrogen atoms omitted for clarity. Color code: Si = green, Gd = orange, C = gray.

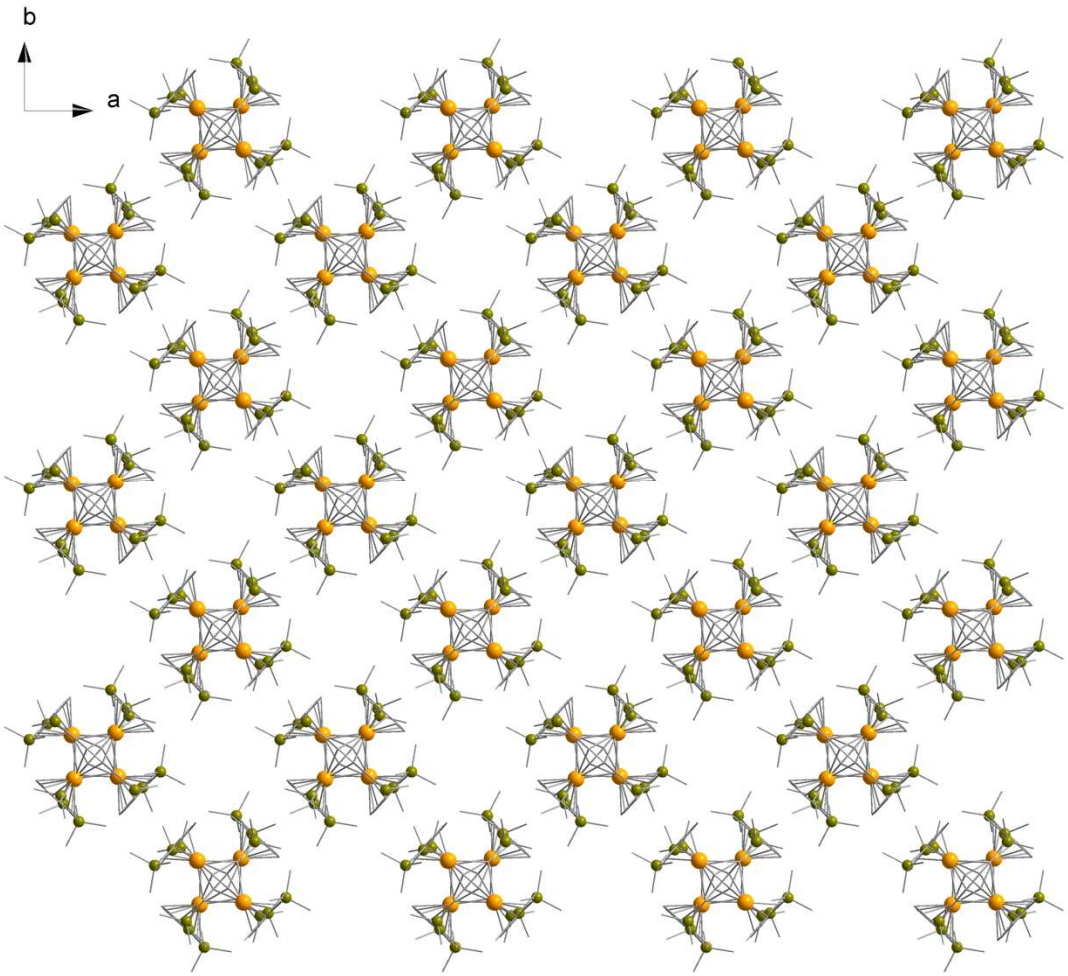

Figure S13: Packing arrangement of **3** looking down the *c* axis. Hydrogen atoms omitted for clarity. Color code: Si = green, Gd = orange, C = gray.

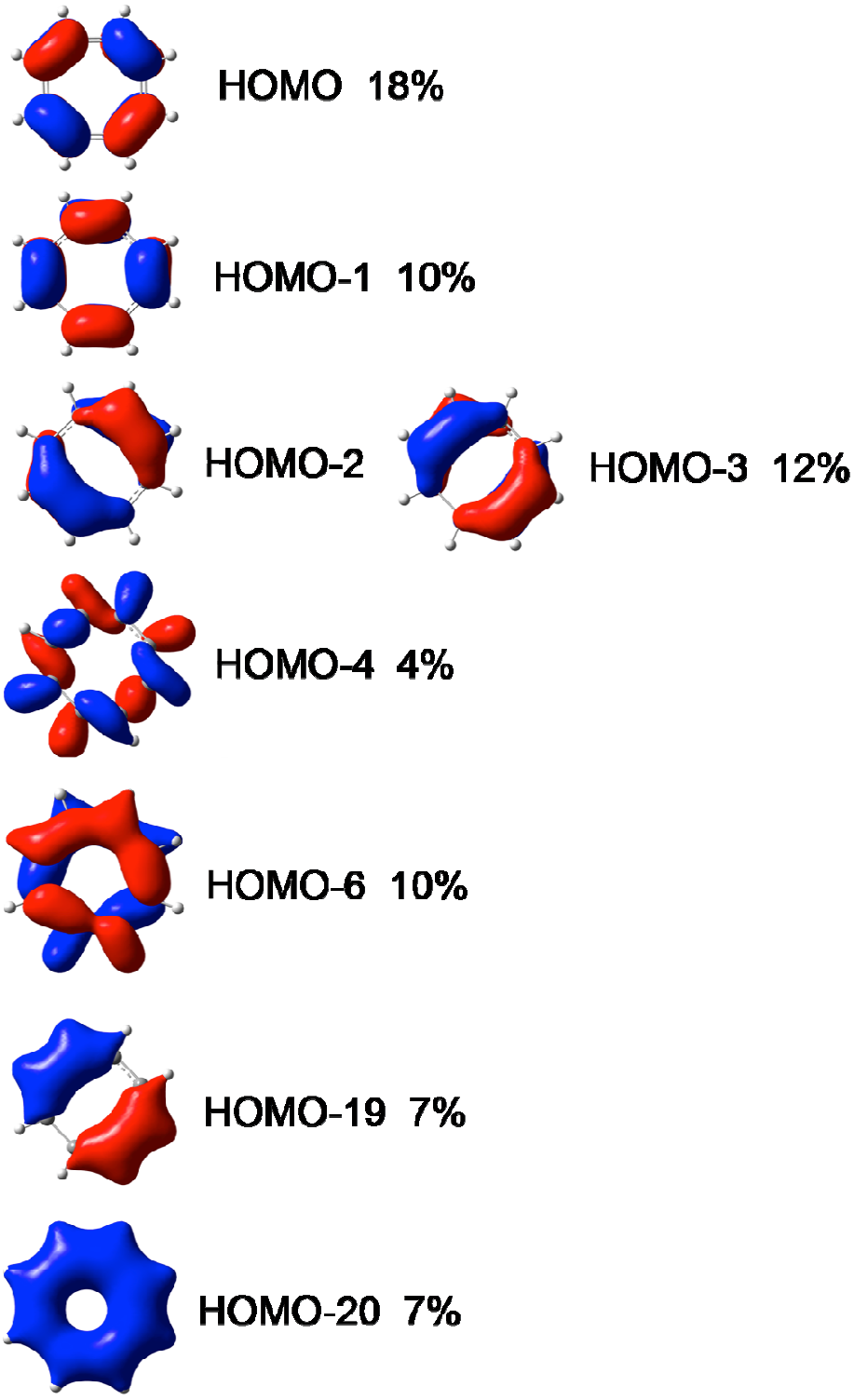

Figure S14: Fragment molecular orbitals of the central COT'' dianionic ligand that contribute significantly (>3% change in occupancy) to the bonding in the $Dy_2(COT'')_3$ complex. % Changes in occupancy upon bonding in the complexes are shown. Isosurface value of 0.04 was used for visualization of the orbitals.

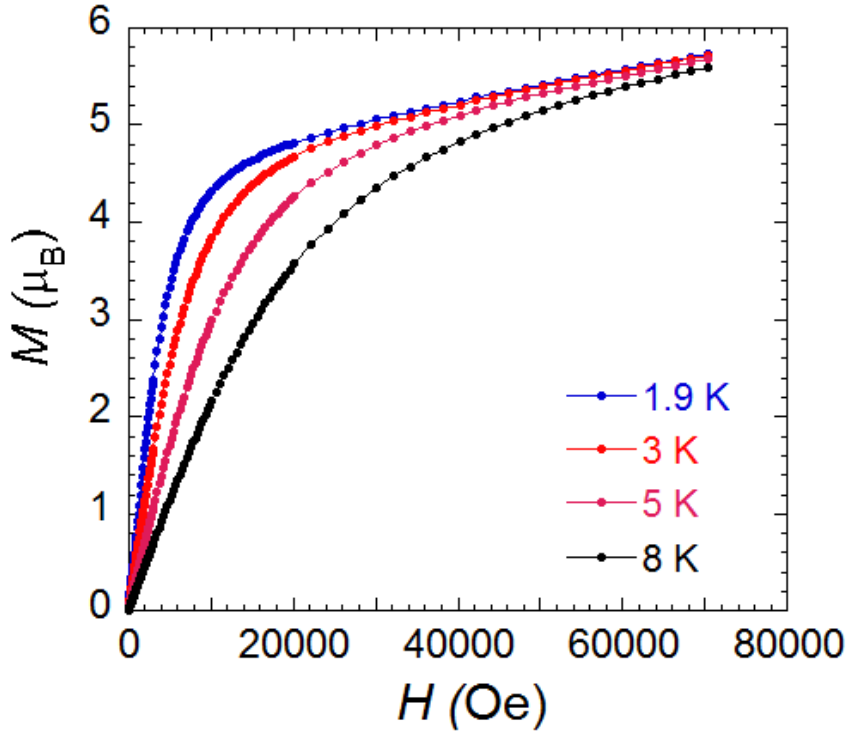

Figure S15: Field dependence of the magnetization for **1** at 1.9, 3, 5, and 8 K.

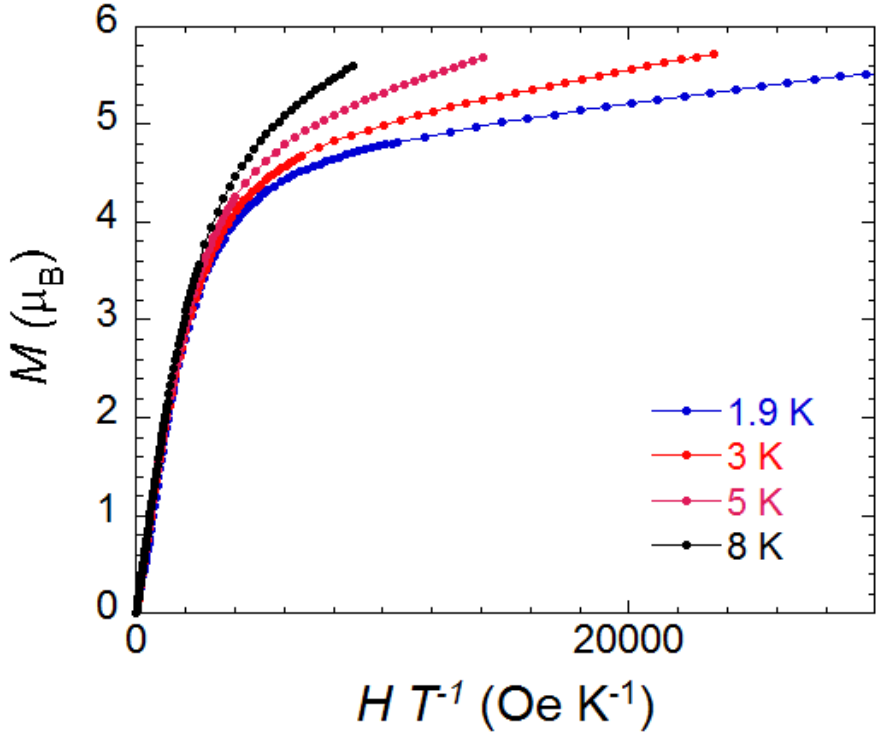

Figure S16: *M vs. H/T* plot for **1** at indicated temperatures.

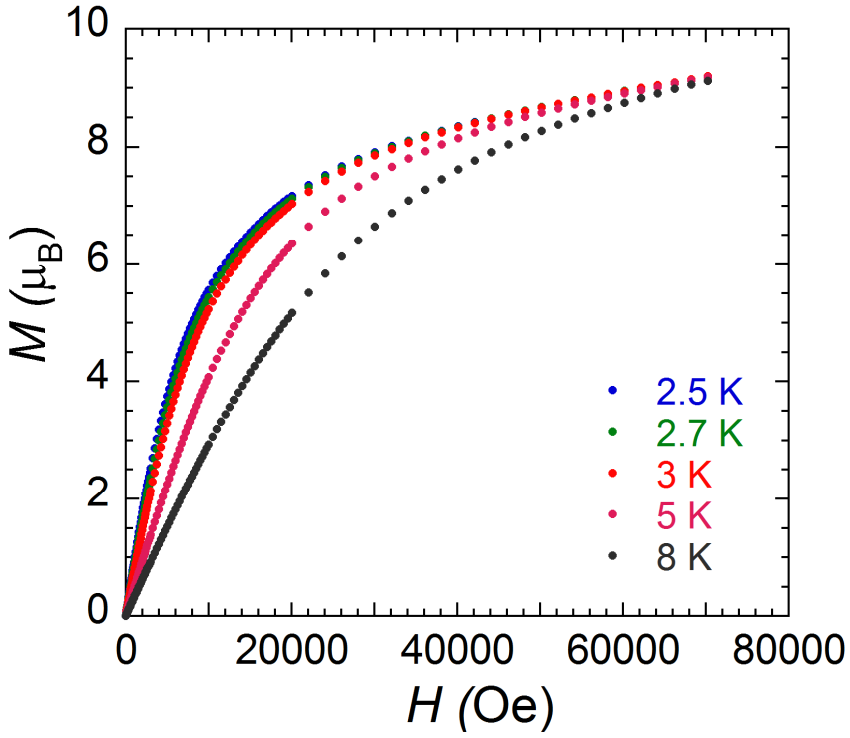

Figure S17: Field dependence of the magnetization for **2** at 2.5, 2.7, 3, 5, and 8 K.

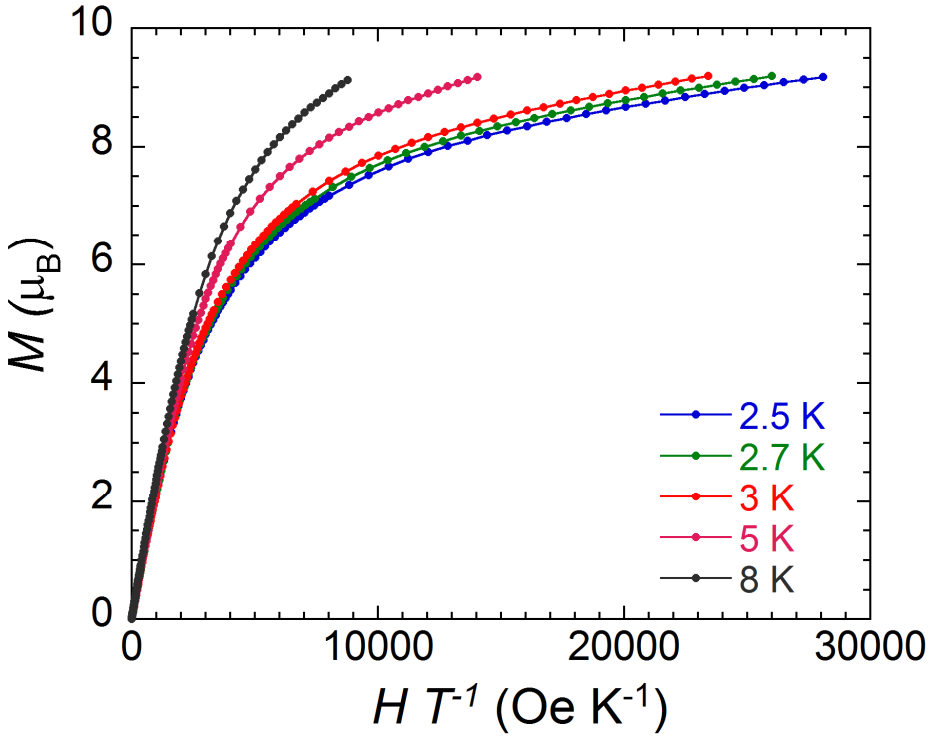

Figure S18: *M vs. H/T* plot for **2** at indicated temperatures.

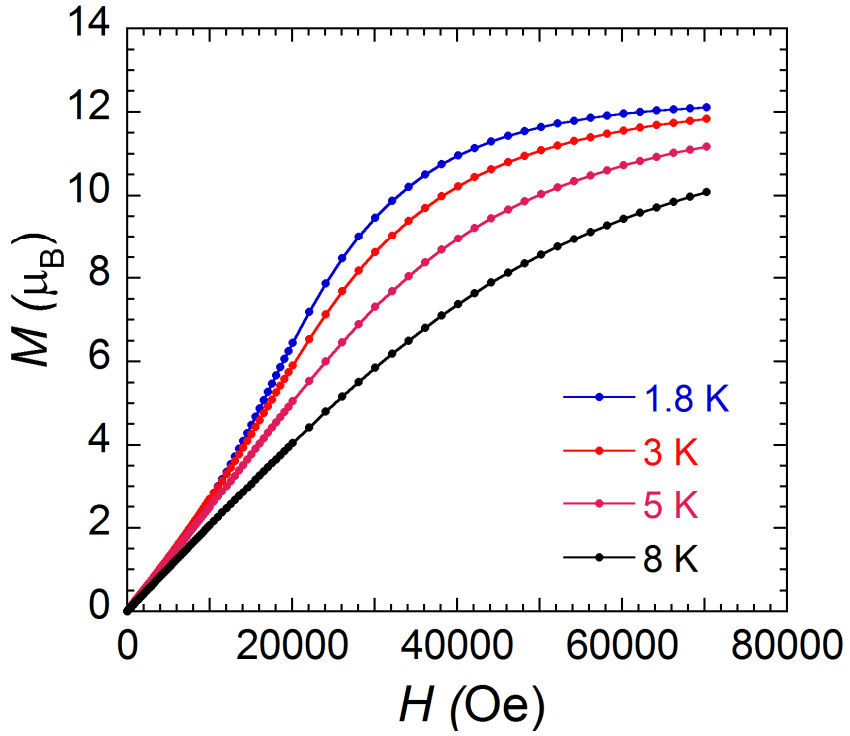

Figure S19: Field dependence of the magnetization for **3** at 1.8, 3, 5, and 8 K.

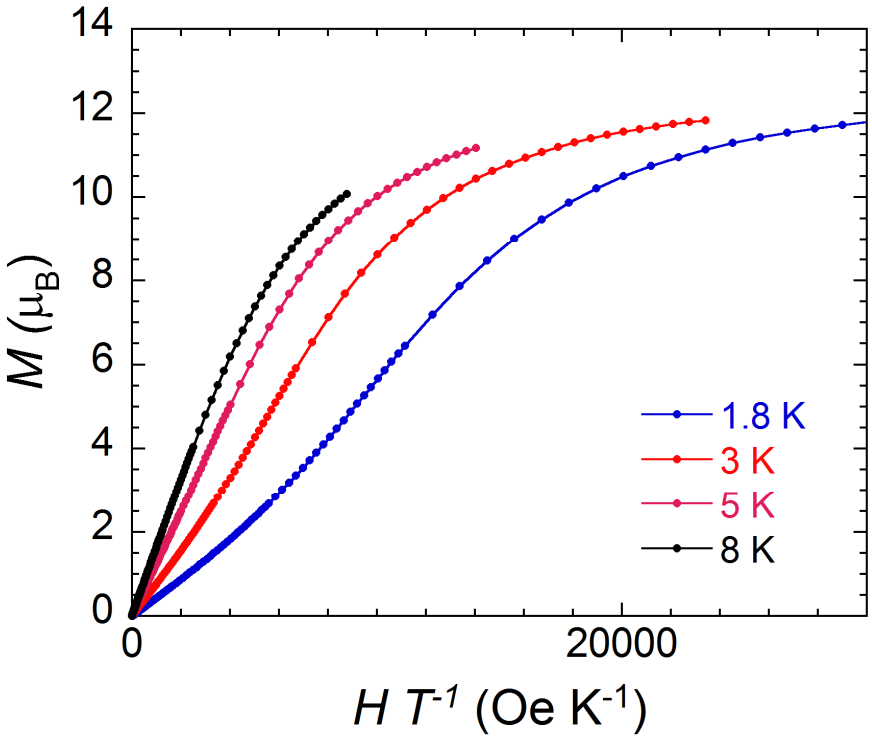

Figure S20: *M vs. H/T* plot for **3** at indicated temperatures.

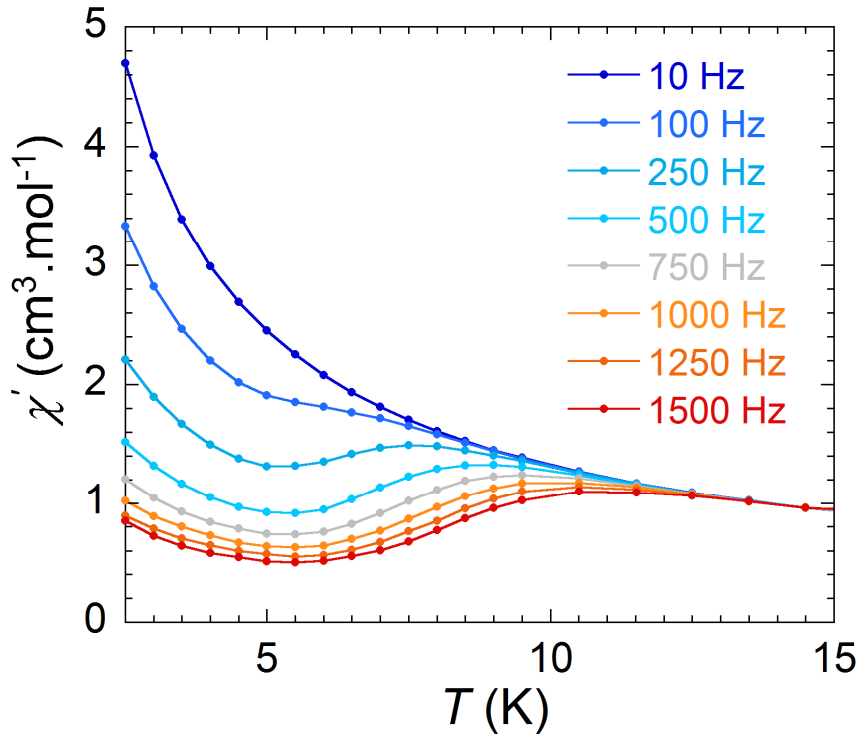

Figure S21: Temperature dependence of the in-phase (χ') magnetic susceptibility at indicated frequencies under zero applied dc field at indicated frequencies (Hz) for **1**.

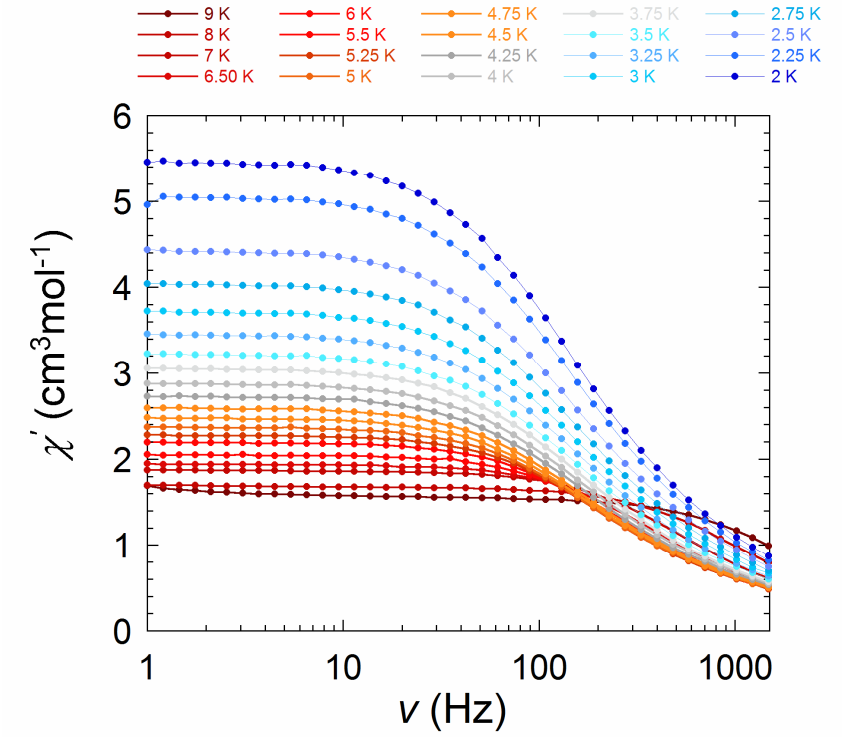

Figure S22: Frequency dependence of the in-phase (χ') magnetic susceptibility at indicated temperatures of **1** under zero applied dc field.

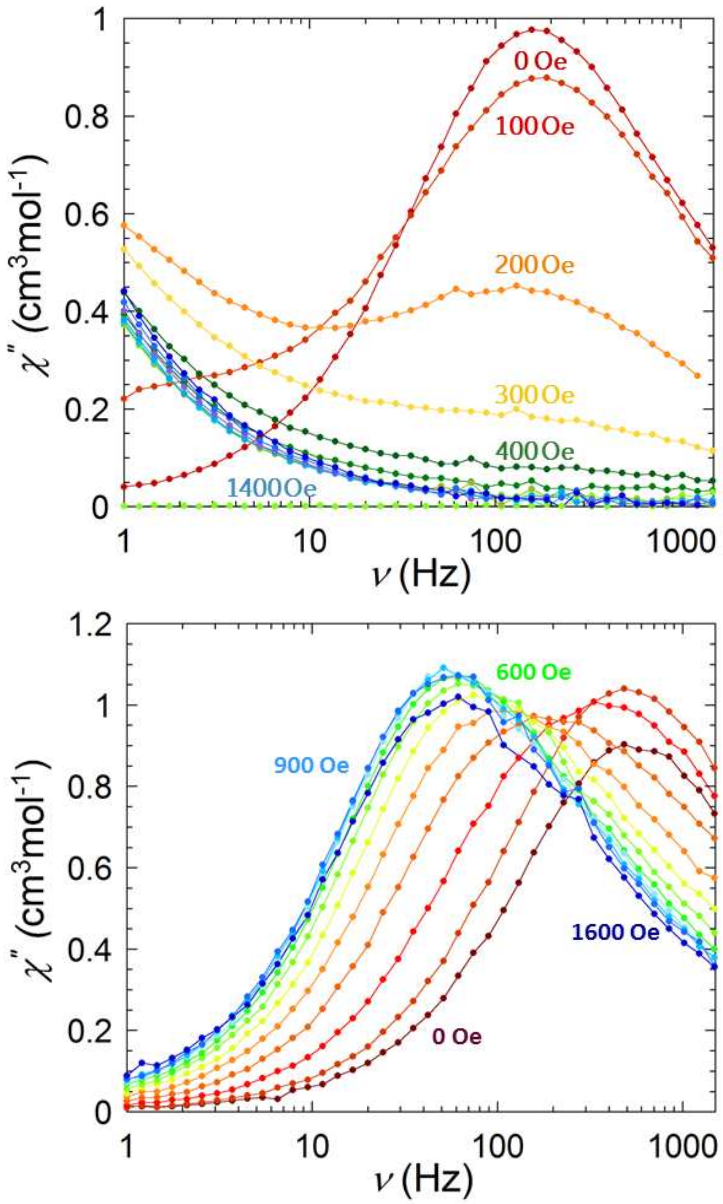

Figure S23: Frequency dependence of the out-of-phase (χ") magnetic susceptibility of **1** (top) and **2** (bottom) under fields between 0-1600 Oe, at 3K.

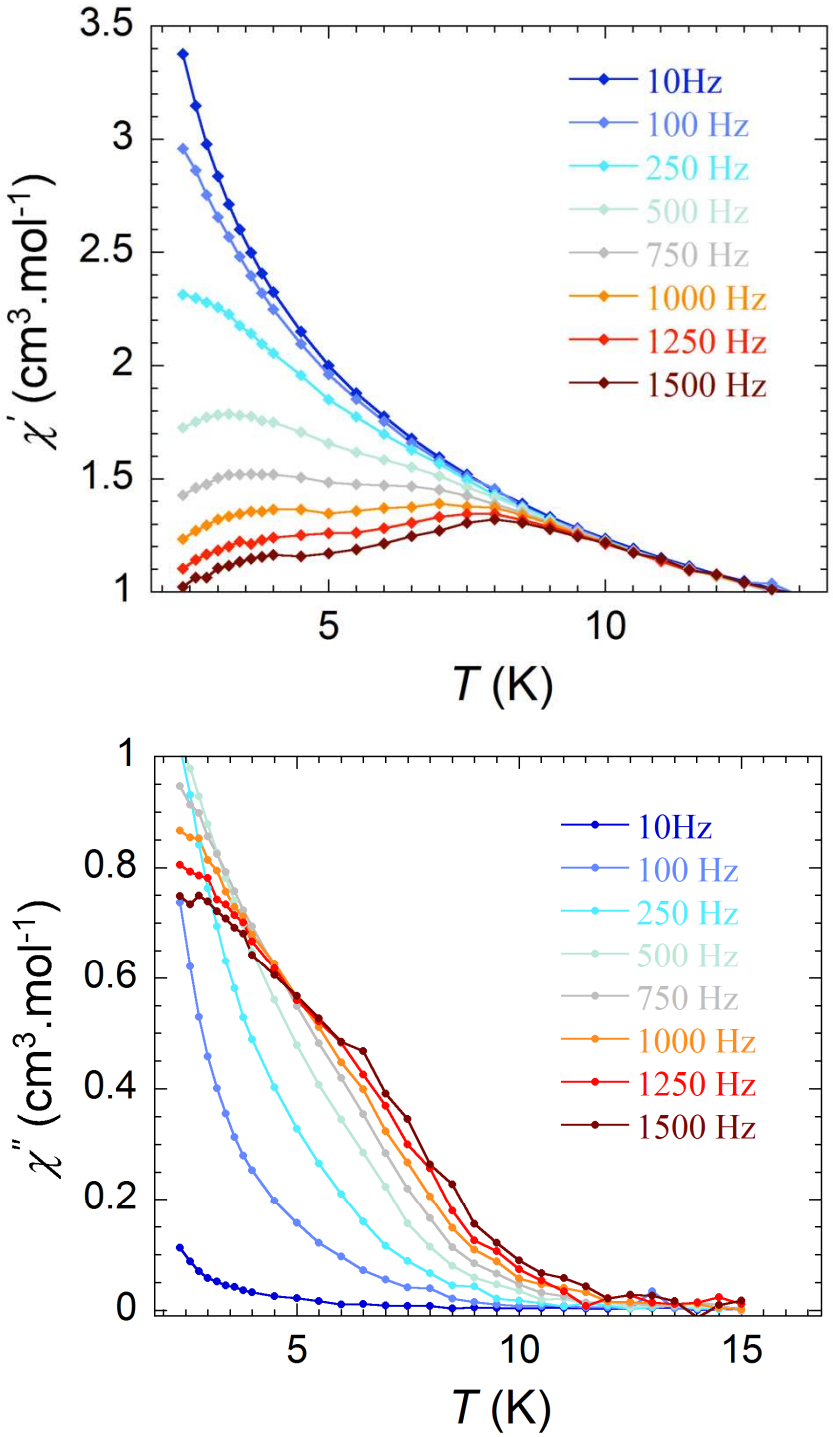

Figure S24: Temperature dependence of the in-phase (top), and out-of-phase (bottom) magnetic susceptibility of **2** at indicated frequencies under zero applied dc field.

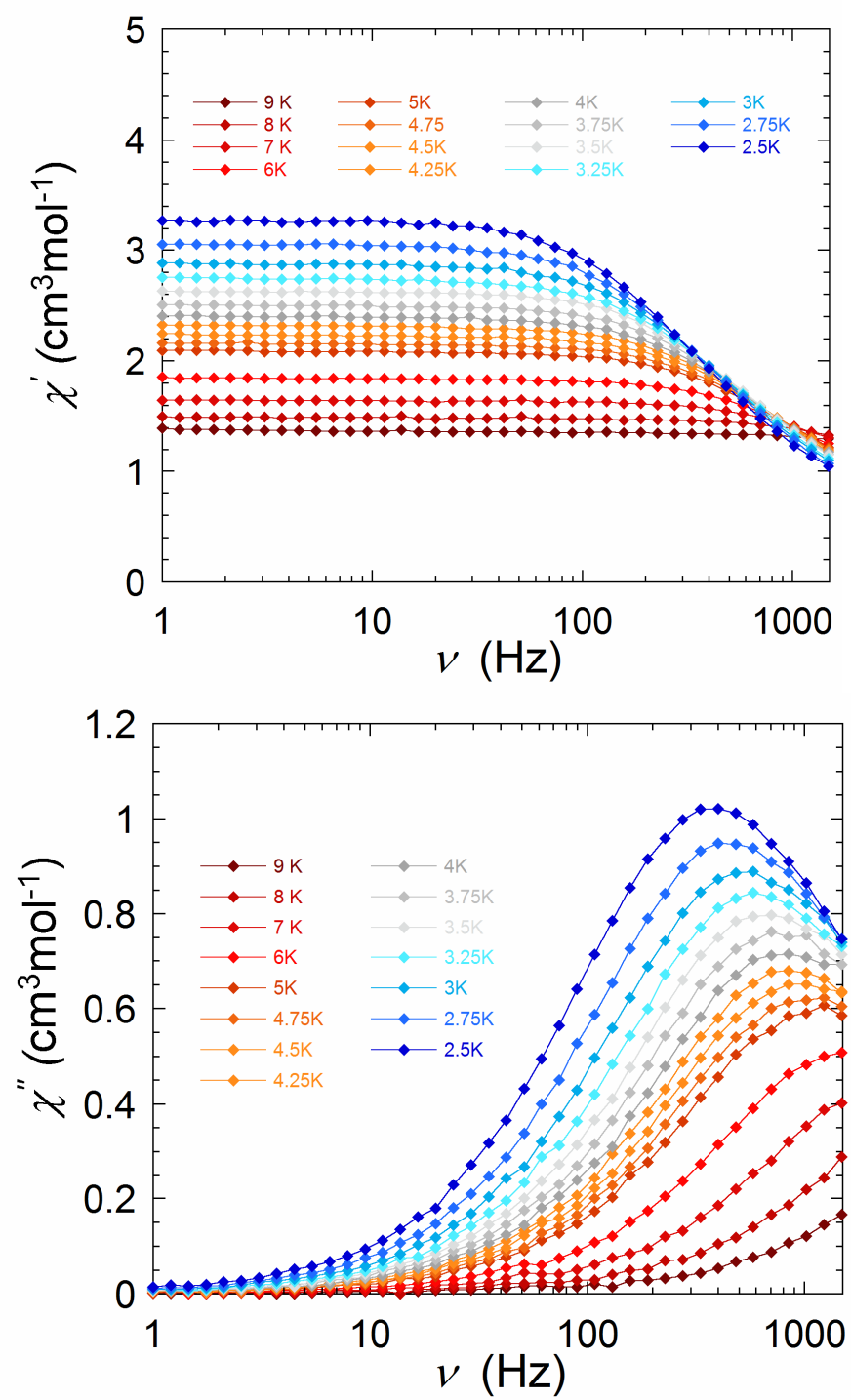

Figure S25: Frequency dependence of the in-phase (top) and out-of-phase (bottom) susceptibility of **2** at indicated temperatures under zero applied dc field.

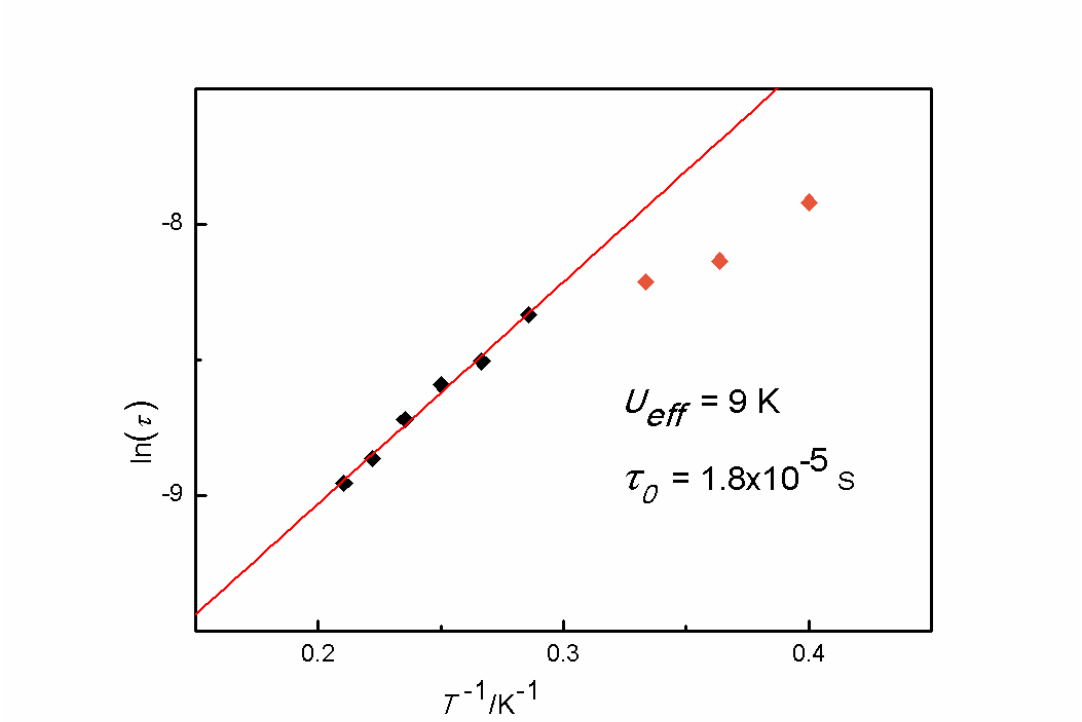

Figure S26: Relaxation time of the magnetization ln(τ) *vs*. T^{-1} for **2** (Arrhenius plot using ac data) under zero applied field. The solid line corresponds to the fit.

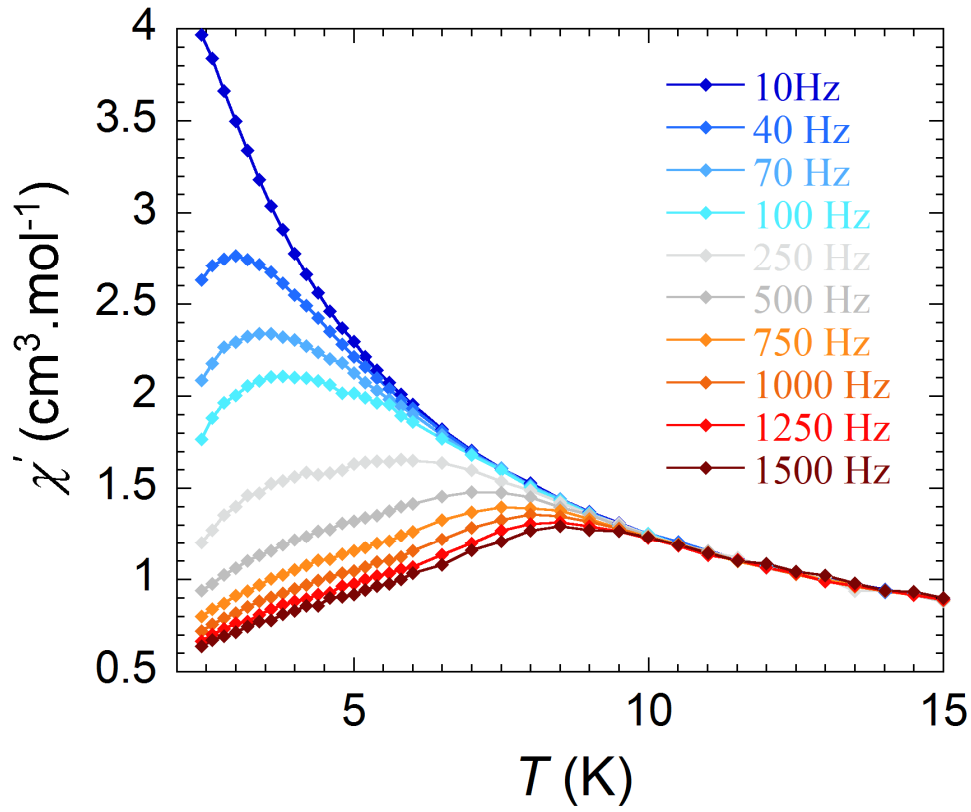

Figure S27: Temperature dependence of the in-phase (χ') susceptibility of **2** at indicated frequencies under 600 Oe applied dc field.

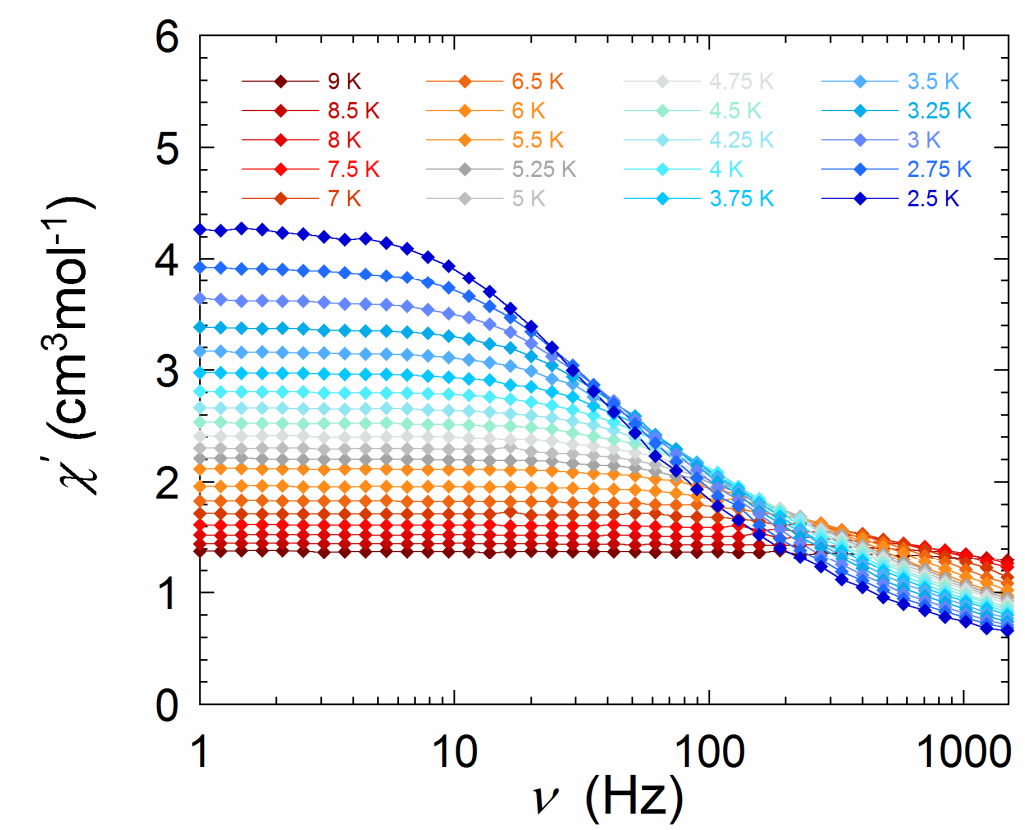

Figure S28: Frequency dependence of the in-phase susceptibility (χ') of **2** at indicated temperatures under a 600 Oe applied dc field.

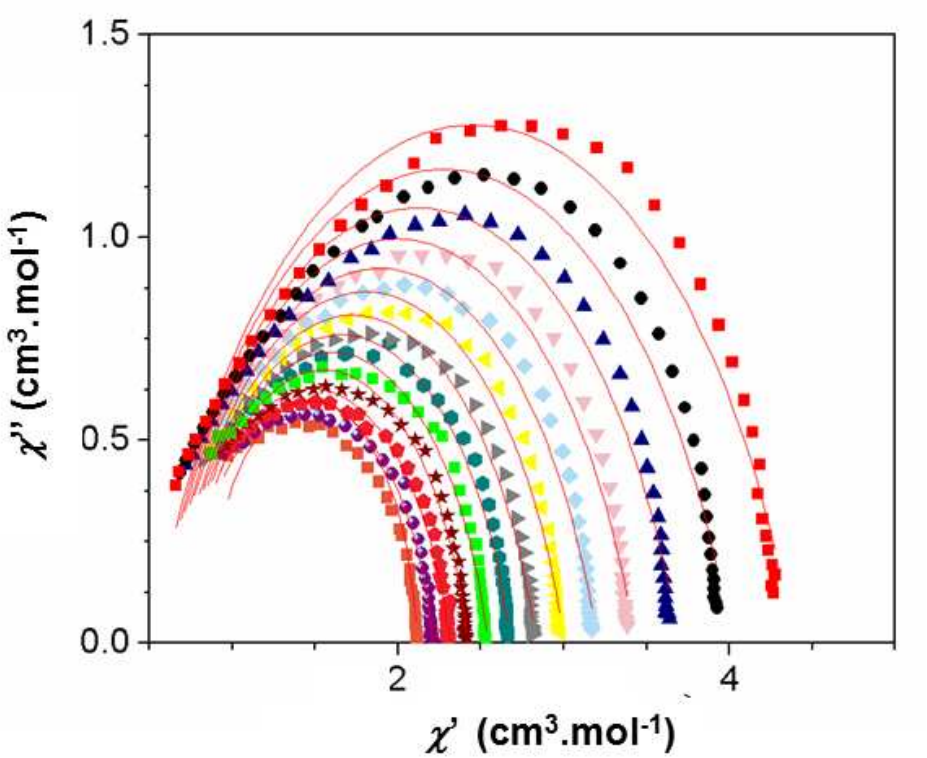

Figure S29: *Cole-Cole* plot for **2** at 600 Oe, solid lines correspond to the attempetd fit.

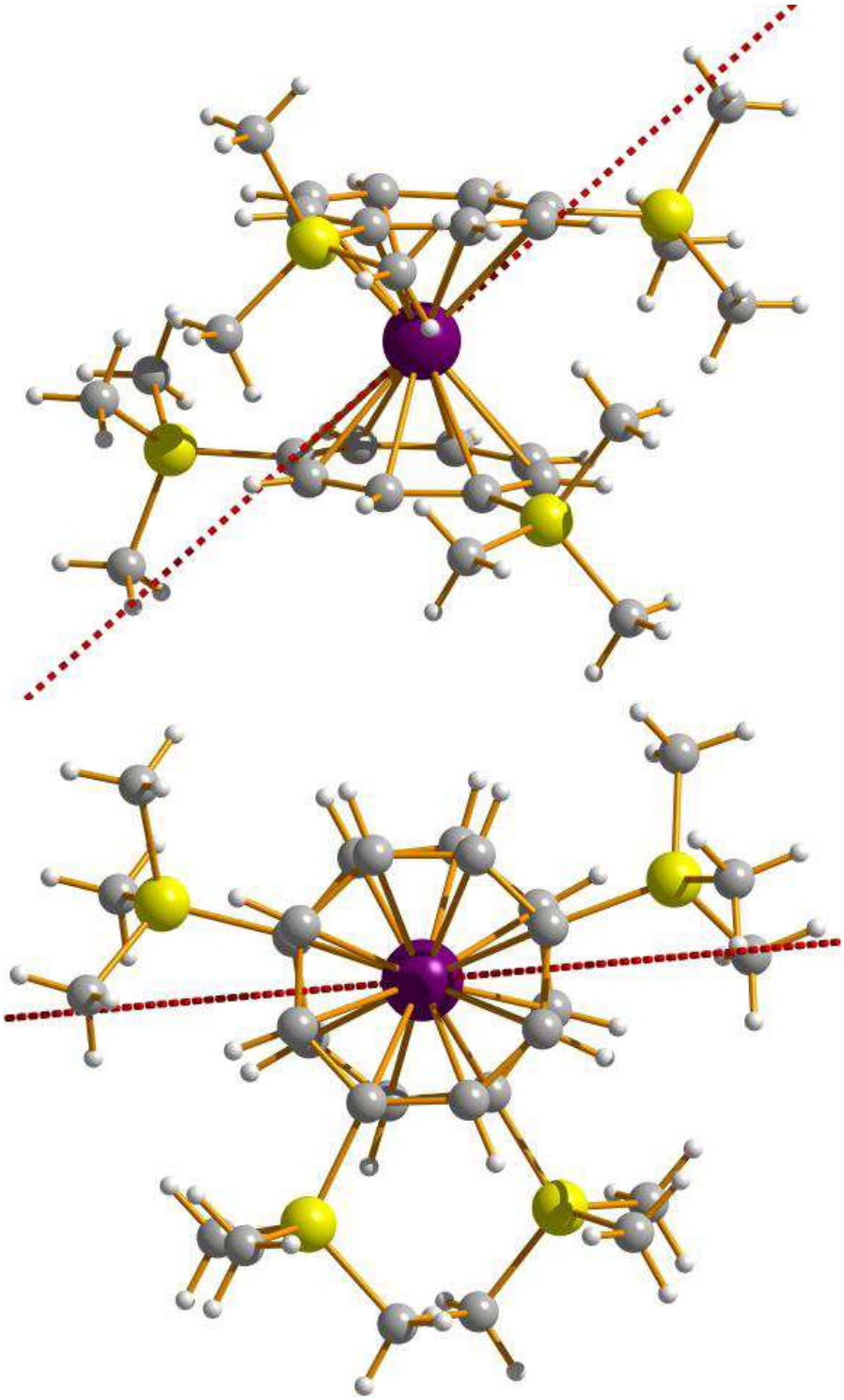

Figure S30. Orientation of the main anisotropy axes in the ground Kramers doublet of $[Dy(COT)_2]^-$.